ISSN 0003-701X, Applied Solar Energy, 2020, Vol. 56, No. 5, pp. 309–323. © Allerton Press, Inc., 2020.
Russian Text © The Author(s), 2020, published in Geliotekhnika, 2020, No. 5, pp. 437–453.

DIRECT CONVERSION OF SOLAR ENERGY INTO ELECTRICAL ENERGY

Application of Modified MPPT Algorithms: A Comparative Study between Different Types of Solar Cells

D. Khodair[a, b], M. S. Salem[c, d], A. Shaker[e], H. E. Abd El Munim[f], and M. Abouelatta[a, *]

[a] *Department of Electronics and Electrical Communications, Faculty of Engineering, Ain Shams University, Cairo, 11517 Egypt*
[b] *Department of Engineering Physics, Faculty of Engineering and Technology, Future University, Cairo, Egypt*
[c] *Department of Computer Engineering, Computer Science and Engineering College, University of Ha'il, Ha'il, Saudi Arabia*
[d] *Department of Electrical Communication and Electronics Systems Engineering, Faculty of Engineering, Modern Science and Arts University, Cairo, Egypt*
[e] *Department of Engineering Physics and Mathematics, Faculty of Engineering, Ain Shams University, Cairo, 11517 Egypt*
[f] *Department of Computer and Systems Engineering, Faculty of Engineering, Ain Shams University, Cairo, 11517 Egypt*
**e-mail: m.abouelatta@eng.asu.edu.eg*

Received October 10, 2019; revised May 27, 2020; accepted July 3, 2020

Abstract—Due to the broad needs for energy as market demands, searching on how to improve the efficiency of the PV systems is an essential concern for researchers to worry about. So, it is crucial to force the PV system to work at its peak power point in order to get the maximum available power from the photovoltaic panel. This paper presents a comprehensive comparison between four Maximum Power Point Tracking (MPPT) Algorithms; Perturb and Observe (P&O), Incremental Conductance (INC), Modified Variable Step Size Perturb and Observe (M-VSS-P&O) and Modified Variable Step Size Incremental Conductance (M-VSS-INC) by using of the DC-DC boost converter for three different kinds of solar cells. These cells are polycrystalline KC200GT cell, monocrystalline shell SQ85 cell and thin film shell ST40 cell. Simulations have been performed using MATLAB-SIMULINK for the three types of solar cells to investigate their performance under both standard test conditions (STC) and slowly varying and sudden changes in solar irradiance. The study has considered the response time, output power efficiency and steady-state-oscillations. The simulation results of the modified algorithms show an improvement in the cell performance in steady state conditions, tracking time and boost converter efficiency as well as an enhancement in the dynamic response in tracking the maximum power point (MPP) in varying climatic conditions over conventional algorithms.

Keywords: polycrystalline, monocrystalline, thin film, photovoltaic, perturb and observe, incremental conductance, maximum power point tracking

DOI: 10.3103/S0003701X20050084

1. INTRODUCTION

Searching for sustainable and renewable energy sources becomes an urgent need due to the fade of fossil resources. Among the different alternative resources, solar energy is the most desirable and popular one because of its reliability, abundantly [1, 2], and its effective rule in decreasing the global warming problem.

Using photovoltaic (PV) systems offer several advantages [3]. Simply, they can be an important source of clean energy by reducing fuel use and consequently decreasing air pollution [4]. More advantages include their low required maintenance to produce energy and their lower prices [5]. Recently, PV panels were used in many applications, such as battery chargers, water pumping systems, solar water heaters [6], seawater desalination [7], constructing buildings with zero energy consumption [8] and it can be used also for aeronautical applications [9]. The principle of the PV panel is based on the photovoltaic effect, which converts the incident light from the sun into electricity [10]. So, the output energy of the panel is affected by solar irradiation and temperature, which leads to a nonlinear behavior [11].

Further, this output energy is also influenced by the internal parameters of the panel [12, 13]. Therefore, an enhancement of this source of energy is a considerable concern of researches seeking to extract the maximum available power from the PV panel, especially in unstable climatic weather conditions with high reliability and lower cost [14]. In order to do that, different solutions have been previously discussed in the literature. The major solution proposed in the literature to overcome this challenge is the maximum power point tracking (MPPT) controller that must be added to the photovoltaic system to maximize power extraction under all conditions. These algorithms,

used in MPPT, differ in many aspects such as cost, effectiveness, response time, steady-state oscillations, accurate tracking in case of a sudden change in temperature or solar irradiance and partial shading condition and implementation complexity [15, 16].

Different MPPT algorithms have been proposed in [17], such as Fractional Short-Circuit Current (FSCC), Fractional Open-Circuit Voltage (FOCV) [18], Fuzzy Logic Control (FLC) [19], Artificial Neural Network (ANN) [20], Perturb and Observe (P&O) [17] and Incremental Conductance (INC) [17].

The most extensively standard commercialized MPPT algorithms used in tracking are Perturb & Observe (P&O) [21, 22] and incremental conductance (INC) [23, 24], due to their easy implementation and medium complexity as they need low requirements in hardware and sensors. However, with these advantages, P&O algorithm has main drawback, as it presents some oscillations around the MPP because perturbations in the control signal are continuously changed in both directions to maintain the MPP position. Also, it can make an incorrect decision in perturbation direction in case of rapid change in the incident irradiance level increasing power losses [25, 26]. So, different approaches and implementations for the P&O algorithm were proposed to overcome the limitations of the traditional P&O. As in [25], the classical constant duty cycle perturbation has been replaced by a Δd that reduces linearly with the increase of the power drawn from the PV field combined with further refinement of the technique. Meanwhile, an adaptive P&O MPPT algorithm with faster dynamic response and improved stability according to validated numerical simulations and experimental tests has been proposed in [26] to adapt the perturbation amplitude to the actual operating conditions. Another different implementation of P&O to improve the efficiency of the system using embedded microcontroller-based real-time with combined of hardware-in-the-loop (HIL) and embedded C language were proposed in [27, 28].

Moreover, the incremental conductance (INC) algorithm with fixed step size was proposed with the objective of minimizing the oscillation around the desired maximum power point by comparing the slope of the $P–V$ curve with zero at the MPP hoping to have the ability to track the MPP during dynamic changes of solar irradiations [29]. Meanwhile, INC operates complicatedly compared with P&O because it employs several division computations that need a timely calculation process and a stronger microcontroller to use [24]. So, the algorithm responds with low speed when fixed step size is used. Moreover, P&O and INC methods may fail to track the MPP, when solar irradiation is rapidly changed [15] or partial shading occurs. Therefore, there was a necessity for some modifications to be presented for INC algorithm, which found to be a right solution for the enhancement of the panel output power and to eliminate the division computations as in [9]. In addition, modified approaches of INC algorithms that can overcome the confusion faced by the conventional INC technique associated with the dynamic response to the various environmental conditions were proposed in [30, 31]. However, despite the previous modifications done for both conventional algorithms as presented earlier in the literature, some of them are not able to respond faster and accurately to the first step change in the duty cycle under rapid environmental changes [24].

To validate the performance of such MPPT algorithms, it is required to test them under different operating conditions. However, it is difficult to realize the desired test case because we cannot control the climatic conditions [32]. MATLAB-Simulink [33] and different simulation environments [28, 34] are used to implement and verify the performance of MPPT algorithms instead of hardware implementation.

In this current study, we present and discuss the results of the simulations carried out using MATLAB-Simulink to prove the effectiveness of two modified algorithms; Modified Variable Step Size Perturb and Observe (M-VSS-P&O) and Modified Variable Step Size Incremental Conductance (M-VSS-INC) in tracking the Maximum Power Point (MPP) under both Standard Test Conditions (STC) and different variations of climatic conditions and its ability to overcome the drawbacks of the conventional algorithms; (P&O and INC) regardless the type of the photovoltaic (PV) panel.

This paper is structured as follows. Following the introduction, Section 2 presents the modeling of PV panel using a single diode model. Section 3 presents the design of the boost converter. The modified algorithms are discussed in Section 4. Section 5 presents the results and discussions and the final section is devoted to the paper conclusion.

2. MODELING OF PHOTOVOLTAIC PANEL

The MPPT system general configuration is shown in Fig. 1. The main objective is to track the maximum power point (MPP) of the panel and forcing it to work at that point [16]. As seen in Fig. 1, the maximum power point of any PV varies with the variation of the atmospheric conditions (solar irradiance and temperature). This means that there is always one optimum terminal voltage for the PV array to operate at with each situation to obtain the maximum power out of it i.e. increase the array's efficiency.

DC-DC converters play an important role in the maximum power point tracking process. As by connecting the array's output terminals with the DC-DC converter's input terminals, the array voltage can be controlled by varying the duty cycle of the converter

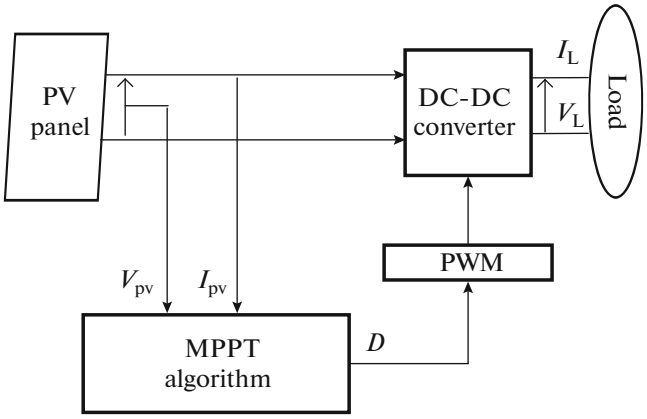

Fig. 1. MPPT system general configuration.

and the voltage at which maximum power can be maintained.

The PV cell is the main component in the photovoltaic panel. In order to meet the practical needs, panels are connected in parallel or series or in both ways to get appropriate output voltage or current from the PV panels depending on how these panels are connected. Putting the cells in series groups will provide higher voltage, while connecting them in parallel gives higher current. Different PV models have been proposed in the literature to serve several purposes [35, 36].

For simplicity, the single-diode model of the PV panel is used in this work as it can provide a good combination between accuracy and simplicity, which considered an effective model for the simulation of PV panels with power converters [37].

2.1. Mathematical Model

The basic structure of the single diode model shown in Fig. 2 can be modeled by a DC photocurrent source in parallel with an ideal diode and a series and a parallel resistances R_s and R_{sh}, respectively. The values of these two resistors are obtained through measurements made from the characteristic of the cell [10, 38, 39].

Based on the equivalent circuit of PV panel, the output generated current can be calculated by [40],

$$I_{pv} = I_{ph} - I_s\left(e^{\left(\frac{V_{pv}-I_{pv}R_s}{AV_T}\right)}-1\right)-\frac{V_{pv}-I_{pv}R_s}{R_{sh}}, \quad (1)$$

where

$$V_T = \frac{kT}{q}. \quad (2)$$

With I_{ph} is the photocurrent which depends mainly on the radiation and cell's temperature, I_s is the diode's reverse saturation current (A), A is the diode

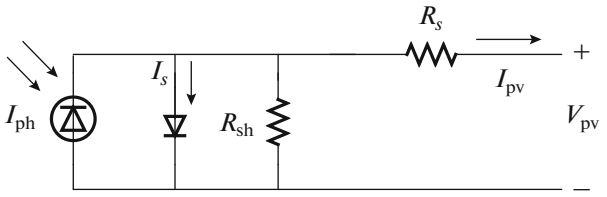

Fig. 2. Single-diode model equivalent circuit of a PV module.

ideality factor, q is the electron charge (1.6021×10^{-19} C), V_T is the thermal voltage, T is the junction temperature in Kelvin, and k is the Boltzmann constant (1.3865×10^{-23} J/K).

For an accurate PV model, I_{ph} calculated by Eq. (3) and I_s computed using Eq. (4) need to be adjusted carefully, as they are used to estimate the values for R_s and R_{sh} that affect the produced maximum power point by the panel using parameter estimation method based on the three major points in the PV panel characteristic [38],

$$I_{ph} = \frac{G}{G_{STC}} - \left(I_{sc} + K_i\left(T - T_{STC}\right)\right), \quad (3)$$

$$I_s = \frac{I_{sc} + K_i\left(T - T_{STC}\right)}{e^{\left(V_{oc}+\frac{K_V(T-T_{STC})}{AV_T}\right)}-1}, \quad (4)$$

where G is the irradiance (W/m^2), STC is the standard test condition (1000 W/m^2 and 25°C), G_{STC} is the irradiance under STC (1000 W/m^2), K_i is the temperature coefficient of I_{SC}, T_{STC} is the temperature under STC (25°C), and K_V is the temperature coefficient of V_{oc}.

2.2. Models Specifications

This work discusses three different types of solar cell modules; polycrystalline, monocrystalline and thin film solar cells. The manufacture's specification list for the three types are mentioned in Table 1 measured at STC. V_{oc} is the open circuit voltage, I_{sc} is the short circuit current, V_{mp} is the voltage at the maximum power point, I_{mp} is the current at the maximum power point, K_V is the temperature coefficient of the open circuit voltage, K_i is the temperature coefficient at the short circuit current and N_s is the number of cells per module.

All modules are simulated according to the electrical parameters given in Table 1 under STC. The I–V and P–V characteristics are presented in Fig. 3 for the three modules. As shown in P–V curves, the desired point where the power drawn from the panel is at its highest value called the maximum power point (MPP).

These characteristics curves are totally influenced by the incident solar irradiance and temperature. So, a

Table 1. Electrical specifications for the PV modules at standard test conditions (STC)

Type	Polycrystalline KC200GT	Monocrystalline Shell SQ85	Thin film Shell ST40
V_{oc} , V	32.9	22.2	23.3
I_{sc}, A	8.21	5.45	2.68
V_{mp}, V	26.3	17.2	16.6
I_{mp}, A	7.61	4.95	2.41
K_V, V/°C	–0.123	–0.0725	–0.1
K_i, A/°C	0.00318	0.0008	0.00035
N_s	54	36	36

change in the climatic weather conditions leads to a non–linear PV cell characteristics causing a significant difference in the MPP position. Also, the load exhibits its behavior and affects the MPP. Therefore, it is necessary to involve MPPT algorithm in the photovoltaic systems in order to track and reach the maximum power point under any circumstances.

2.3. Effect of Sun Irradiation and Temperature Variation

To present the impact of temperature and solar irradiance variations, the three PV panels are simulated for different values of irradiance (G) and temperature (T). According to the PV modeling Eqs. (3) and (4), it is apparent that the computed photocurrent is based on both temperature and the incident irradiance, while the diode saturation current is based on temperature only. Therefore, the change in irradiance and temperature has a strong impact on the PV panel output current and voltage. These effects are shown in Figs. 4 and 5.

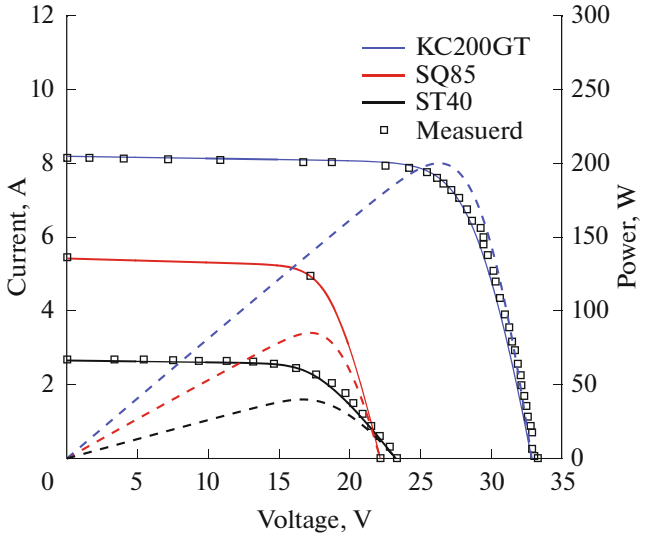

Fig. 3. I–V and P–V characteristics for single-diode model of polycrystalline cell KC200GT, monocrystalline cell SQ85 and thin film ST40.

As presented in Fig. 4, PV panels are simulated for different values of solar irradiance at $T = 25$°C. With a fixed temperature both open-circuit voltage and short-circuit current are directly proportional to the solar irradiation. Thus, the irradiance change strongly affects the PV panel current.

Furthermore, to present the temperature variation effect, PV panels are simulated for different values of temperature at $G = 1000$ W/m^2 and the I–V and P–V obtained characteristics are shown in Fig. 5. It can be inferred that when the temperature increases for fixed solar irradiation, the open-circuit voltage decreases and the short-circuit current increases with a little value. Therefore, the temperature variation affects only the PV panel voltage.

Increasing solar irradiance, the open-circuit voltage increases logarithmically, whereas the short circuit current increases linearly and thus, the output power increases. Temperature plays another major factor in determining the solar cell efficiency. As the temperature increases, the rate of photon generation increases and the bandgap decreases; thus, reverse saturation current increases rapidly. Hence, this leads to marginal changes in current but major changes in voltage. Temperature acts like a negative factor affecting solar cell performance. Therefore, solar cells give their full performance on cold and sunny days rather on hot and sunny weather.

3. BOOST CONVERTER DESIGN

It is difficult to extract the maximum power and regulate the output voltage without a converter. So, in PV systems, a DC-DC converter, controlled by the duty cycle output from the MPPT, must be located between the PV panel and the load to deal with the occurrence mismatches between the load and the MPP during the different environmental conditions. Figure 6 shows the circuit of the DC-DC boost converter (step-up converter) used in this work to boost its input DC voltage (V) to the required output DC voltage level (V_o).

The design of the circuit components is provided as follows. The maximum power point resistance is given by,

$$R_{mp} = \left(\frac{V_{mp}}{I_{mp}}\right). \quad (5)$$

The duty cycle for the peak power transferred at STC is determined by using Eq. (6),

$$\alpha = 1 - \sqrt{\frac{R_{mp}}{R}}. \quad (6)$$

And the output voltage is given by,

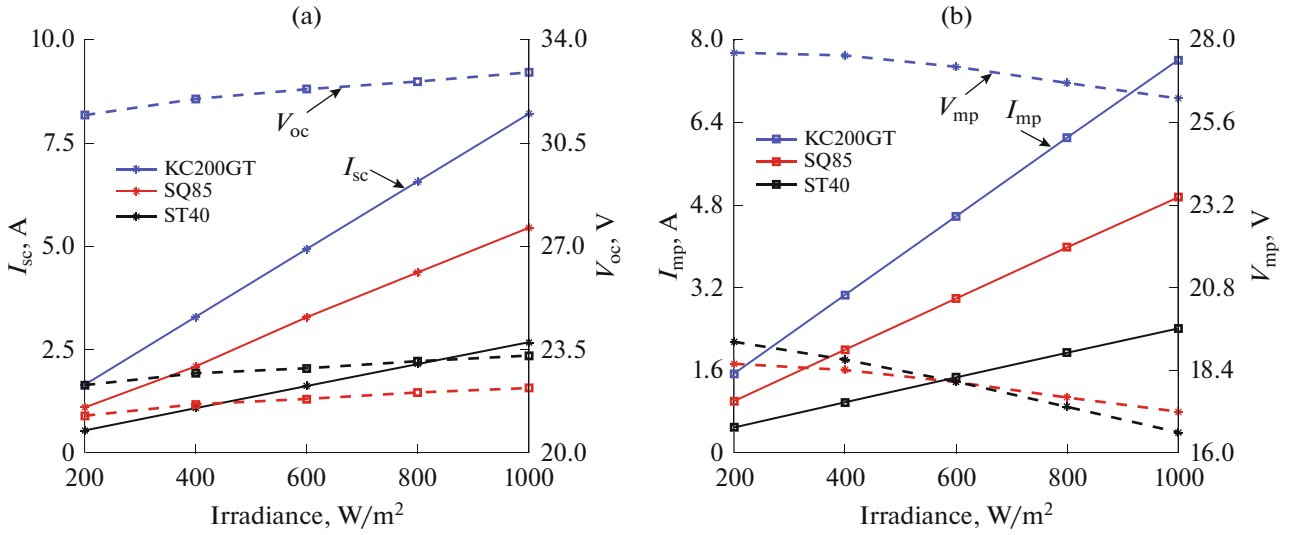

Fig. 4. I_{sc}–V_{oc} and I_{mp}–V_{mp} characteristics for the three different solar modules at different values of solar irradiance and STC.

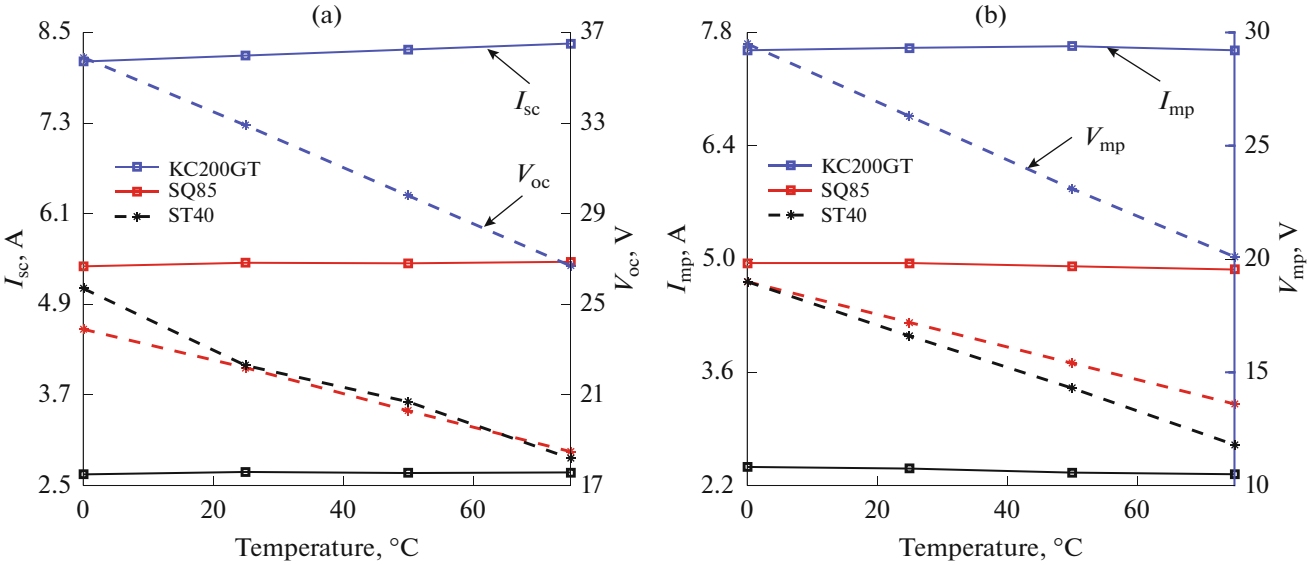

Fig. 5. I_{sc}–V_{oc} and I_{mp}–V_{mp} characteristics for three different solar modules at different values of temperature and 1000 W/m^2 irradiance.

$$V_o = \frac{V}{1-\alpha}, \tag{7}$$

where V is the output voltage from the PV cell.

The output current is evaluated using the following equation,

$$I_o = I(1-\alpha), \tag{8}$$

where I is the output current from the PV cell.

The inductor value can be calculated as mentioned by Eq. (9) where r is between [0.3, 0.5] [41],

$$L \geq \frac{V\alpha}{rIf}. \tag{9}$$

The input capacitor value can be designed as follows,

$$C_1 \geq \frac{\alpha}{8Lf^2 0.01}. \tag{10}$$

The minimum value of the output capacitor can be designed as mentioned by Eq. (11) [24],

$$C_2 \geq \frac{\alpha}{0.02fR}. \tag{11}$$

For a resistive load of 30 Ohm, and according to the above equations [40] given in this section, the parameters used to operate the Boost converter, used in this work, are given in Table 2.

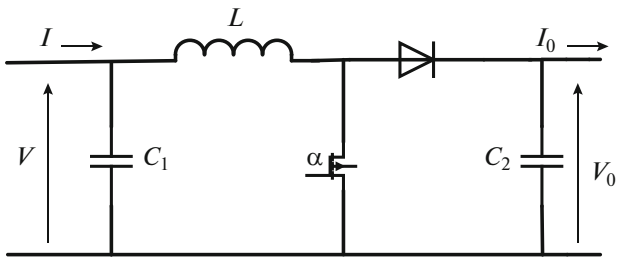

Fig. 6. DC-DC boost converter.

4. MPPT ALGORITHM

The key point for a proper MPPT tracking is to ensure that the input power and output power for the DC-DC converter is the same even though load is changed. Several MPPT techniques have been presented in the literature seeking to locate the maximum power point. As mentioned before, conventional P&O and INC algorithms are the most frequently used techniques because of their simple implementation and medium complexity.

4.1. Problems with the Conventional P&O and INC Algorithms

Both P&O and INC algorithms use the (P–V) characteristic of the PV panel in the tracking process based on the condition that the desired point theoretically reached when $dP/dV = 0$ is accomplished.

But practically, through the real implementation, it is hard to found the zero point on the slope of the power curve because of the truncation error in digital processing as in INC algorithm. So, both techniques were found to be not totally accurate in tracking the MPP due to the resulted steady-state oscillations around the MPP and high response time. The concept of P&O algorithm is based on applying perturbation in the duty cycle in order to change the operating voltage, and then the change in the operating power is observed. Based on this observed value, the next perturbation decision is made. Theoretically, when the algorithm reaches the peak of the P–V curve, there are no additional perturbations added to the duty cycle and the system should respond with no oscillation in the output power. But practically, this principle leads the system to operate near to the MPP but not at the point accurately. As these oscillations are proportional to the offset (step size) and contentious perturbations must be done to preserve the MPP location, oscillations appear after reaching MPP lead to higher oscillations for larger step size and slower tracking with high response time in case of small step size.

Table 2. Boost converter parameters

Parameter	f	C_1	C_2	L	R
Value	10 kHz	100 μF	100 μF	3 mH	30 Ohm

However, the INC algorithm basic idea is depending on using the incremental conductance of the panel to determine the slope of the power curve, and if the incremental conductance is equal to its instantaneous conductance, the MPP can be tracked and no more perturbations are added to the duty cycle. Furthermore, INC process mainly depends on several division computations, so the usage of strong microcontroller is necessary, reducing the chance of using a low-cost development board [30] and taking a longer time to reach the MPP. In addition to these drawbacks presented by both algorithms, they fail to perform and track the maximum point accurately when the solar irradiance is suddenly changed.

4.2. Modified Algorithms

According to the previous discussion, both conventional algorithms are modified to overcome their limitations and the trade-off between faster response and steady-state oscillations associated with the fixed step size. The concept of a variable step size adjustment was presented in the literature [42, 43]. It used a scaling factor depending on the change in both PV power (ΔP) and PV voltage (ΔV). But also, this modification may show poor tracking efficiency in irradiance variations and an increase in the oscillation power [9].

As in the case of stable solar irradiance, ΔV is very low in the area near to MPP and its right region; consequently, the change in ΔP and ΔV is large. So as a result of these large step sizes, the steady state power oscillations is increased. Thereby the algorithm efficiency is decreased.

While, in case of solar irradiance variations especially in the sudden variation, conventional variable step can decrease the performance of the algorithm because the change in the irradiance affects PV current instead of PV voltage so ΔV will be very low whereas there is a significant power variation (ΔP). Consequently, the change ΔP and ΔV is very large. Therefore, the operating point moves far away from the new maximum power point, which in turn increases the time needed to reach new MPP. So, the algorithm efficiency is decreased.

To overcome this limitation, modified MPPTs are designed and implemented following [9] by using of the MATLAB-SIMULINK, based on a modified variable step size, that depends only on the change ΔP with scaling factor adjusted to compromise between the response time and reducing the steady state oscillations to minimize the output PV power oscillations as shown in Figs. 7 and 8.

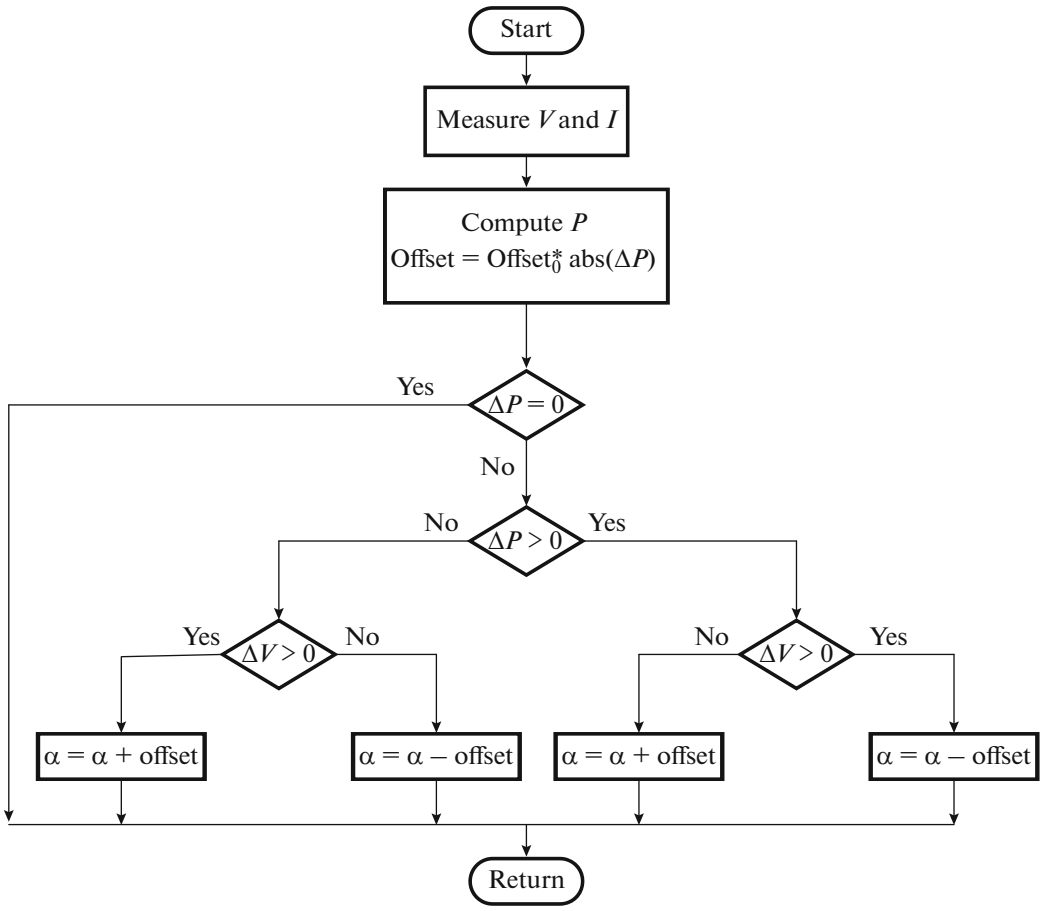

Fig. 7. Modified variable step size P&O (M-VSS-P&O).

5. RESULTS AND DISCUSSION

In this section, steady-state and dynamic performance resulted by using conventional and modified algorithms, P&O, INC, M-VSS-P&O and M-VSS-INC, are investigated for the three types of solar cells (polycrystalline KC200KT, monocrystalline shell SQ85 and ST40 thin film), and tested by using of the MATLAB-SIMULINK. Simulations are presented and analyzed for different variations in solar irradiance (step and ramp change in irradiance) to compare the performance of the algorithms in terms of the response time needed to track the MPP, tracking efficiency and steady state oscillations.

5.1. Test under STC

Figure 9 presents the performance of the polycrystalline cell KC200GT by the four algorithms using. All simulations are conducted under irradiance of 1000 W/m^2 and temperature of 25°C. According to the simulations observed in the figure, both conventional algorithms P&O and INC (65% duty cycle) could reach the peak point with the same output power (198.6 W) with response time (62.7 ms) but with high steady state power oscillations. While using the modified algorithms M-VSS-P&O and M-VSS-INC can improve cell performance.

Both modified algorithms (M-VSS-P&O and M-VSS-INC) can reach the peak point with a much faster response (10.4 ms) and with a better peak power of (199.8 W), with the same duty cycle as both conventional algorithms under STC. As a summery, the performance parameters of a polycrystalline cell KC200GT by the four MPPT techniques using are listed in Table 3.

The same comparative study is conducted on the other monocrystalline Shell SQ85 and thin film Shell ST40 solar cells. Like the earlier case with KC200GT cell, all different algorithms are tested under the same conditions and the modified algorithms show a better performance for both cells. Regarding the monocrystalline Shell SQ85 solar cell, simulations using the four MPPT techniques are presented in Fig. 10 and cell performance parameters are listed in Table 4. While the tracking process of the thin film Shell ST40 is observed in Fig. 11, with its appropriate 51% duty cycle and a summary of the cell performance is illustrated in Table 5.

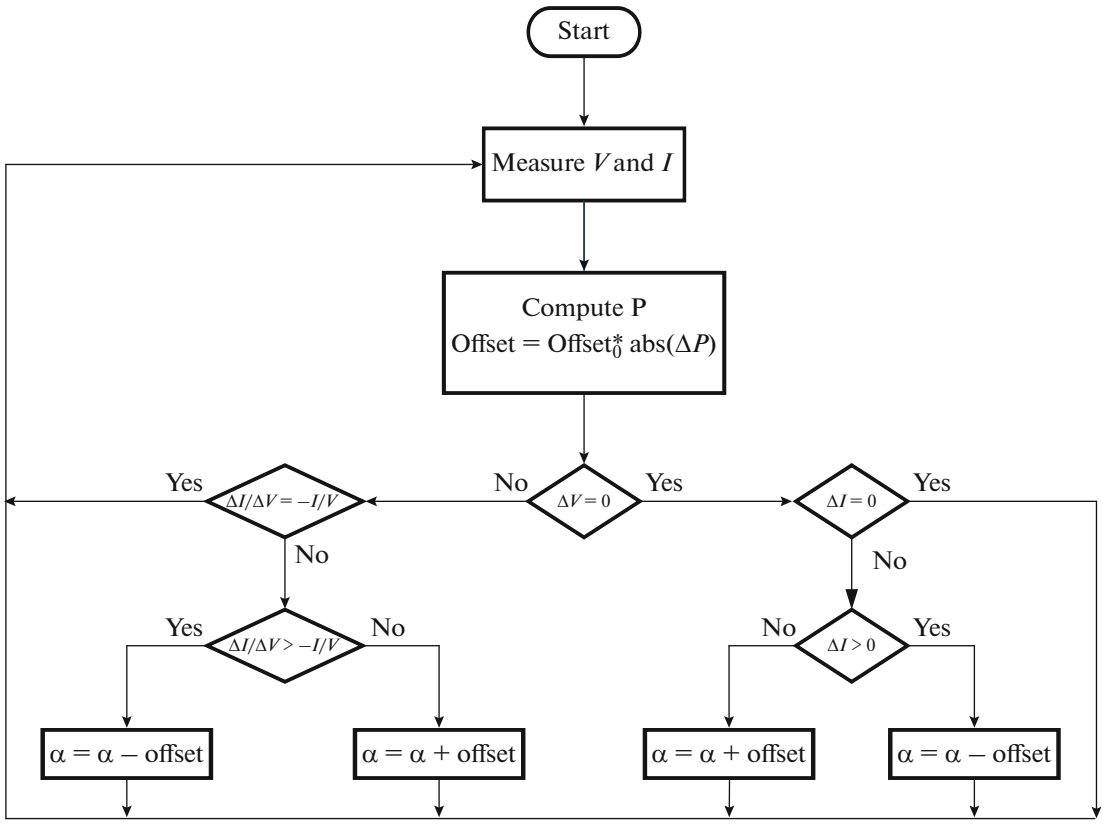

Fig. 8. Modified variable step size INC (M-VSS-INC).

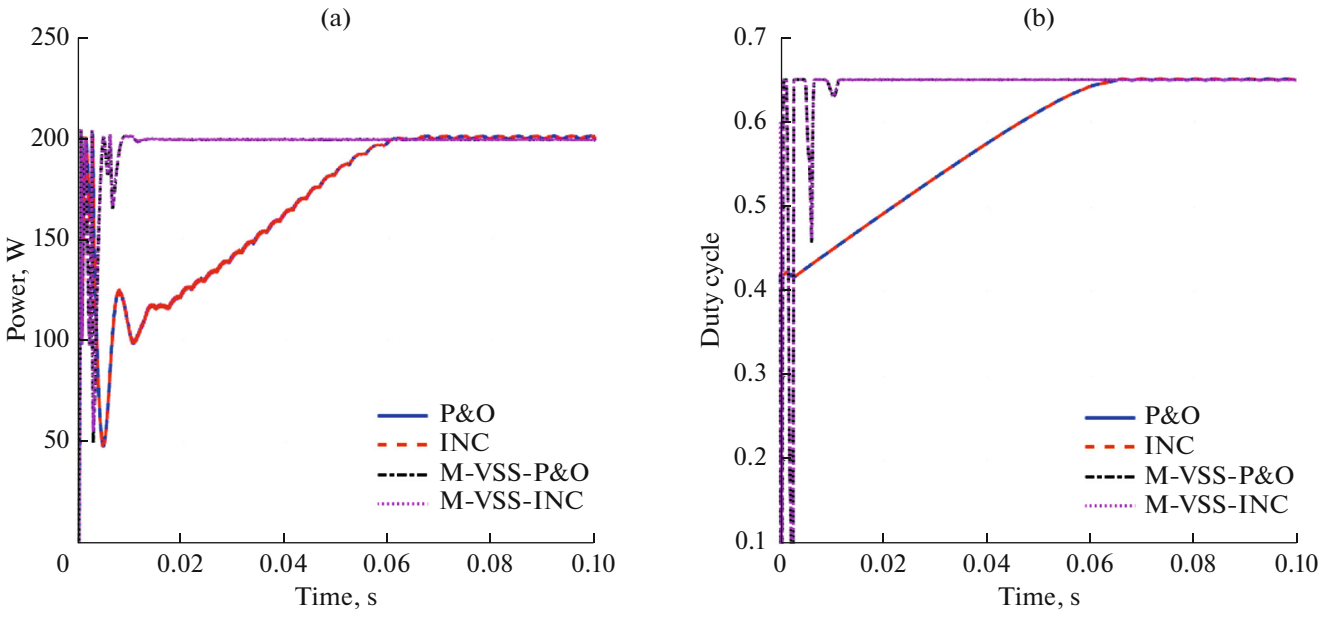

Fig. 9. (a) Performance of polycrystalline KC200GT solar cell, (b) corresponding duty cycle, under STC.

From the above simulations and performance parameters listed in the previous tables in the STC test, it can be noticed that the conventional P&O performs with the less efficiency among the three different cells and presents high oscillations to reach the maximum power point. Also, it is observed that INC

Table 3. Comparative study between the MPPT algorithms under STC for the single-diode model of polycrystalline KC200GT cell

MPPT Technique	MPP, W	Power, W	Tracking time, ms	Oscillations, W	Efficiency, %
P&O	200.143	198.6	62.7	1.4	99.22
INC	200.143	198.6	62.7	1.4	99.22
M-VSS-P&O	200.143	199.8	10.4	Neglected	99.82
M-VSS-INC	200.143	199.8	10.4	Neglected	99.82

Table 4. Comparative study between the MPPT algorithms under STC for the single-diode model of monocrystalline shell SQ85 cell

MPPT Technique	MPP, W	Power, W	Tracking time, ms	Oscillations, W	Efficiency, %
P&O	85.14	84.55	61.2	0.5	99.3
INC	85.14	84.55	61.2	0.5	99.3
M-VSS-P&O	85.14	84.97	13.03	Neglected	99.8
M-VSS-INC	85.14	84.97	13.03	Neglected	99.8

algorithm gives the same performance in the tracking process for the MPP as P&O in the polycrystalline and monocrystalline cells. They both reached the MPP with 99.22% boost converter efficiency with response time equal to 62.7 ms in the KC200GT cell. As noticed in the SQ85 observations, they reached the peak point slightly faster than the polycrystalline cell in 61.2 ms with 84.55 W peak power and 99.3% converter efficiency.

However, according to the thin film solar cell simulations, it is noticed that P&O could reach ~99.8% converter efficiency, but INC was slightly faster than the P&O as it takes 33.71 ms to reach MPP of 40.01 W, while P&O algorithm took around 34.19 ms to reach a peak point of 39.92 W.

On the other hand, in both KC200GT and SQ85 cells, modifications done to both P&O and INC MPPT algorithms success to enhance the performance of the solar cell seeking the maximum available power from the panel and reach the MPP faster than the conventional algorithms with lower oscillations level as much as possible. This is obviously appeared in the simulation results of the polycrystalline KC200GT solar cell, as the efficiency of the MPPT increased to 99.82% in 10.4 ms by using of the both M-VSS-P&O and M-VSS-INC, but in the SQ85 monocrystalline

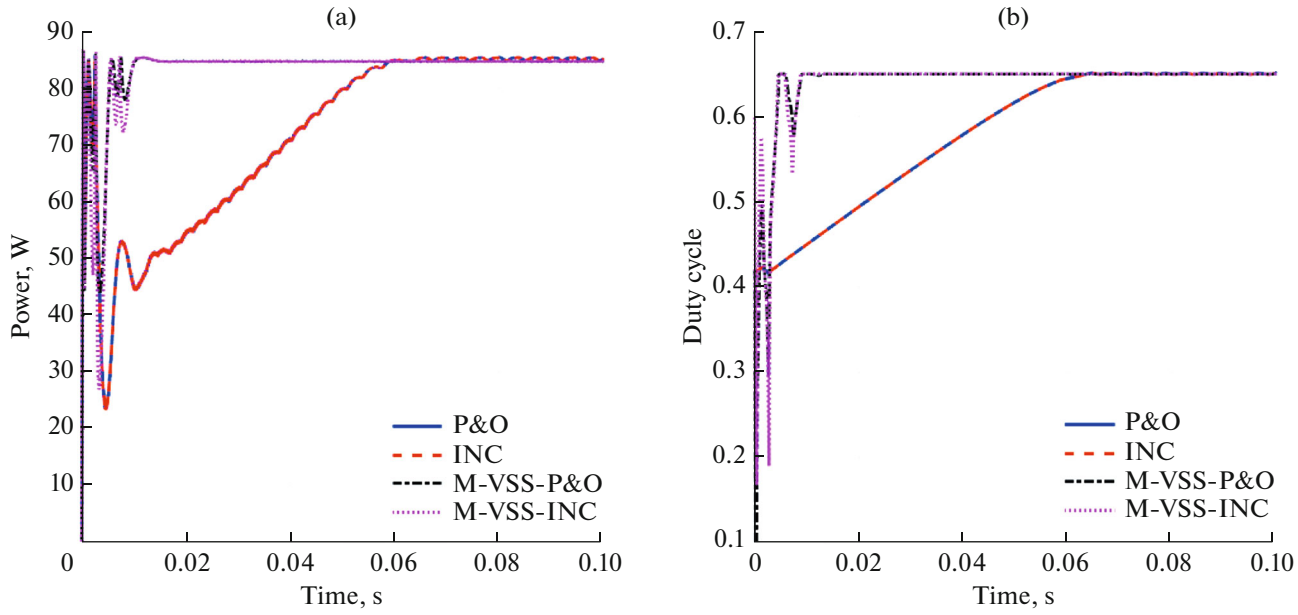

Fig. 10. (a) performance of monocrystalline shell SQ85 solar cell, (b) corresponding duty cycle, under STC.

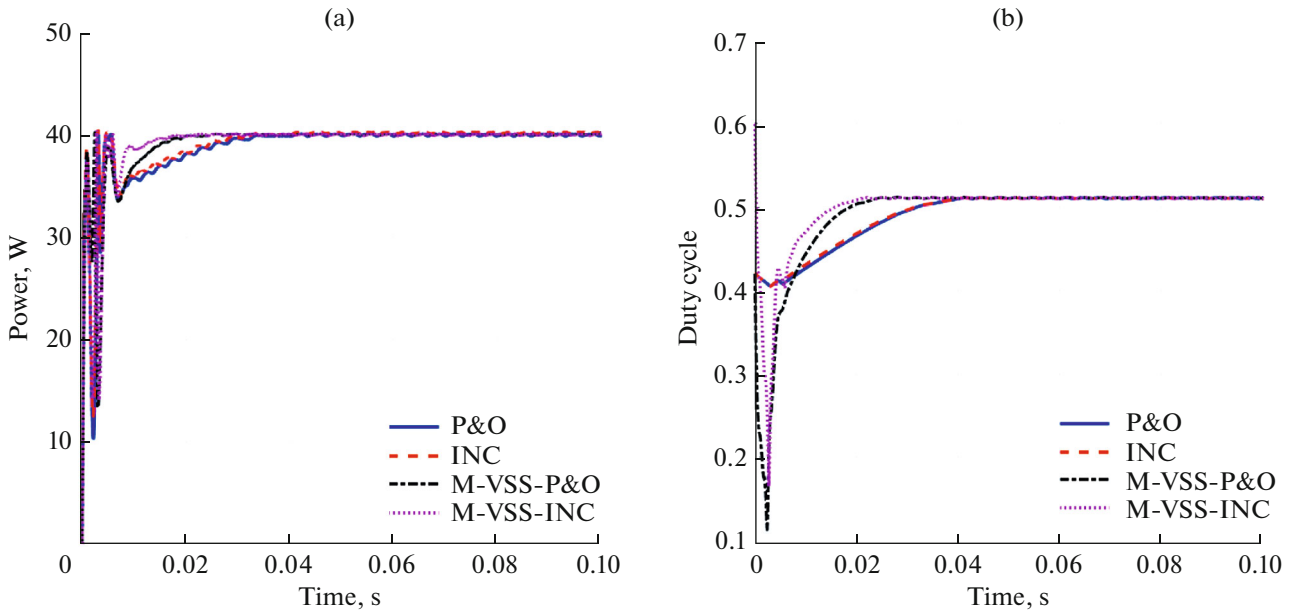

Fig. 11. (a) Performance of thin film ST40 solar cell, (b) corresponding duty cycle, under STC.

cell, both M-VSS-P&O and M-VSS-INC share the same performance to reach the MPP, they success to enhance the cell performance and improve the efficiency to 99.8% and with faster response (13.03 ms) compared to the conventional algorithms with neglected steady state oscillations in both solar cells and also, simulations done using the thin film solar cell show different behavior in tracking. Both modifications reached 100% converter efficiency with (40.2 W) maximum power point and lower oscillation level in faster response time than both P&O and INC, as the M-VSS-P&O could reach the MPP in 26.21 ms and the M-VSS-INC reached it faster in 23.02 ms.

5.2. Test under Sudden Change in Irradiance

To extend our comparative study, two different irradiance changes are tested to each solar cell, as shown in Fig. 12. Firstly, in the sudden change variation test, as shown in Fig. 12a, the irradiance was at 1000 W/m^2 then it suddenly decreased from 1000 to 600 W/m^2 at $t = 5$ s. Then, when the simulation time reached 10 s, a rise in the solar irradiance from 600 to 1000 W/m^2 is applied abruptly and the irradiance maintained constant at 1000 W/m^2 until the end of the simulation time at $t = 15$ s.

Secondly, a ramp change in solar irradiance is done, as seen in Fig. 12b. Here, the irradiance decreased slowly from 1000 to 600 W/m^2 between 2 and 4 s and maintained constant at 600 W/m^2 until it reached $t = 6$ s. after that, a slow increase in irradiance from 600 to 1000 W/m^2 between 6 and 8 s. The simulation time lasts for 10 s.

These simulations are done following [44] to ensure the effectivity of the algorithms to reach the MPP, especially by the modified ones according to different types of solar irradiance change and varying climatic conditions.

In testing the KC200GT cell, as presented in Fig. 13. In case 1, as seen in Fig. 13a, the algorithms performed initially at the STC irradiance as discussed before then, when the irradiance decreased suddenly to 600 w/m^2, both P&O and INC algorithms succeeded in tracking the MPP with much oscillations, showing the same behavior with a response time of 5.026 s; nearly 26 ms error whereas both modified algorithms could converge to the same peak point faster than conventional techniques by the same

Table 5. Comparative study between the MPPT algorithms under STC for single-diode model of thin film Shell ST40 solar cell

MPPT Technique	MPP, W	Power, W	Tracking time, ms	Oscillations, W	Efficiency, %
P&O	40.006	39.92	34.19	0.21	99.78
INC	40.006	40.01	33.71	0.15	100
M-VSS-P&O	40.006	40.02	26.21	0.1	100
M-VSS-INC	40.006	40.02	23.02	0.1	100

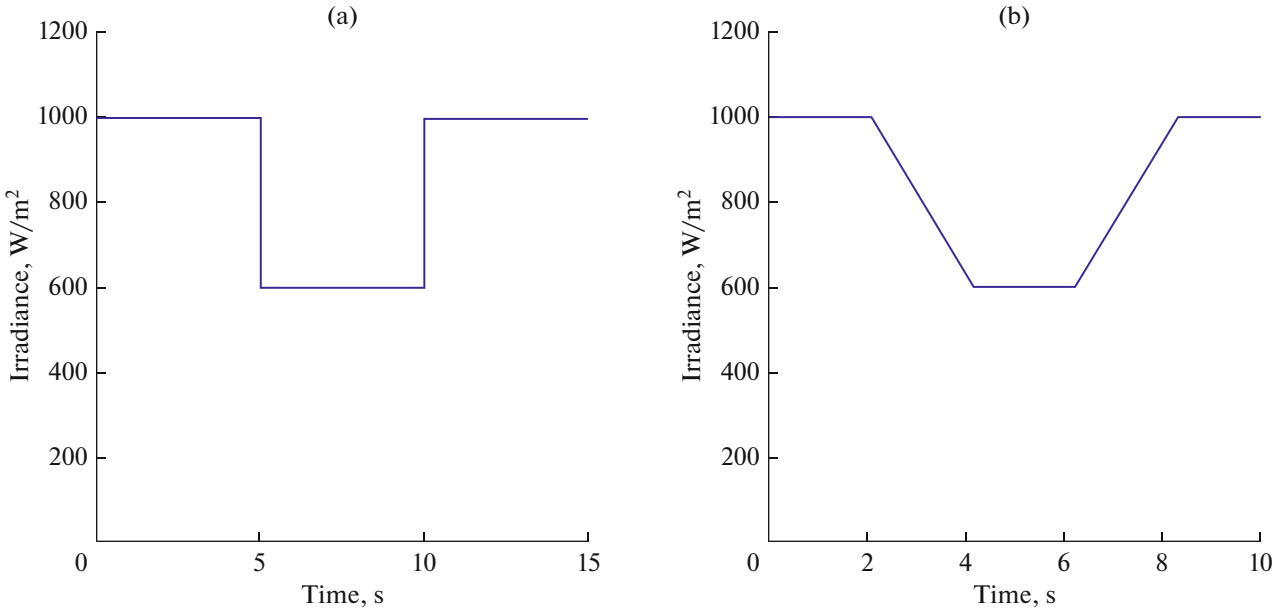

Fig. 12. Different change in solar irradiance: (a) step change, (b) ramp change.

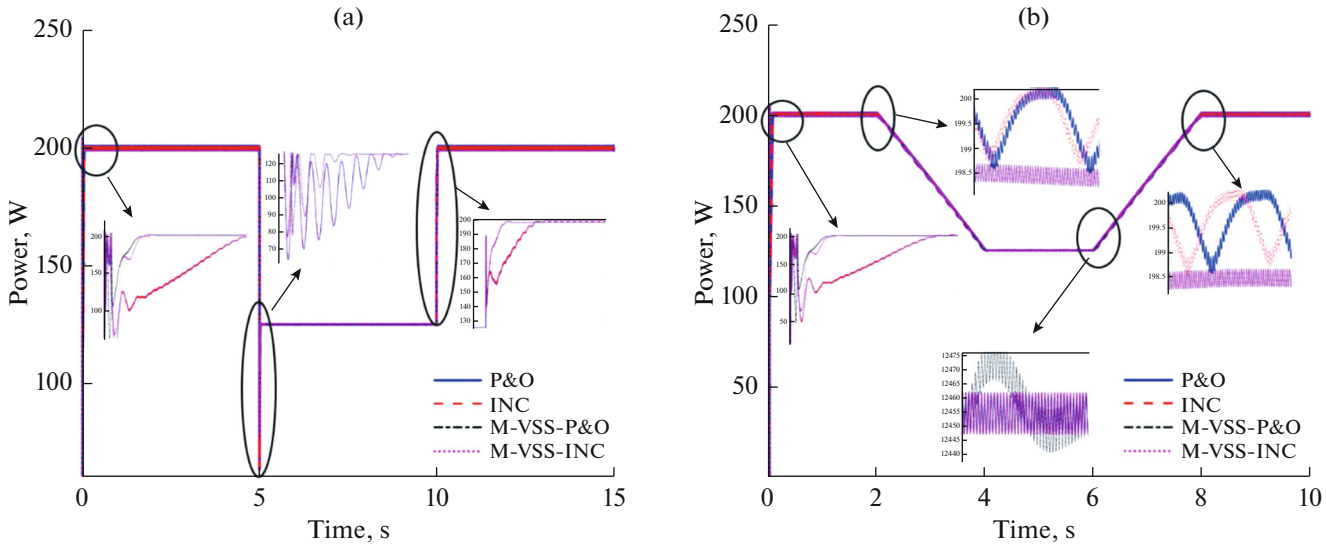

Fig. 13. Performance of polycrystalline cell KC200GT under sudden change in irradiance.

response time of 5.012 s and less error of 12 ms and also could minimize the steady-state oscillations around the MPP. In addition, the modified algorithms could also detect the sudden increase in solar irradiance with only 10 ms error with a slight increase in power from 198.6 W, as submitted by both P&O and INC in 10.03 s to 199.2 W with a quicker reaction.

The output power curves of the four MPPT techniques with ramp change in solar irradiance are shown in Fig. 13b. It can be noticed that the output power of the improved MPPT techniques changes with smaller oscillation than the power of the other conventional MPPT methods.

Similarly, the SQ85 cell performance is presented in Fig. 14. It is observed that the four MPPT algorithms could reach the MPP when the irradiance was suddenly decreased and with around 20 ms error by the modified algorithms. On the other hand, when the irradiance increased suddenly, the modified algorithms could also detect the MPP faster with 84.7 W and only 10 ms error with a minimum level of oscillations. While, both P&O and INC could reach the peak point of 84.55 W after an error of 30 ms. Moreover, as

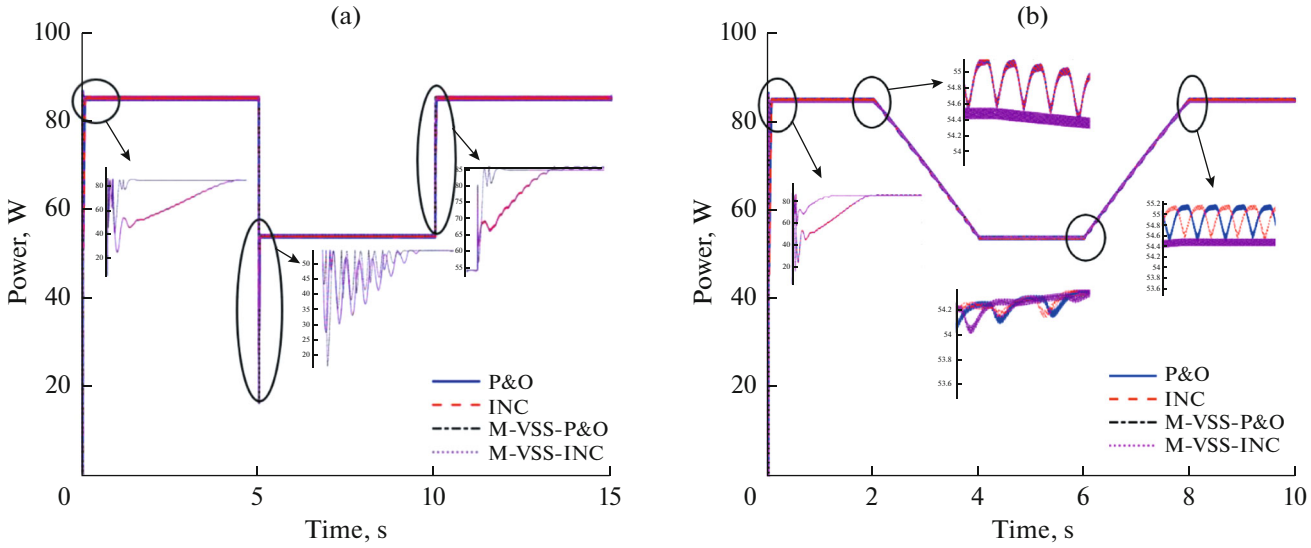

Fig. 14. Performance of monocrystalline cell SQ85 under sudden change in irradiance.

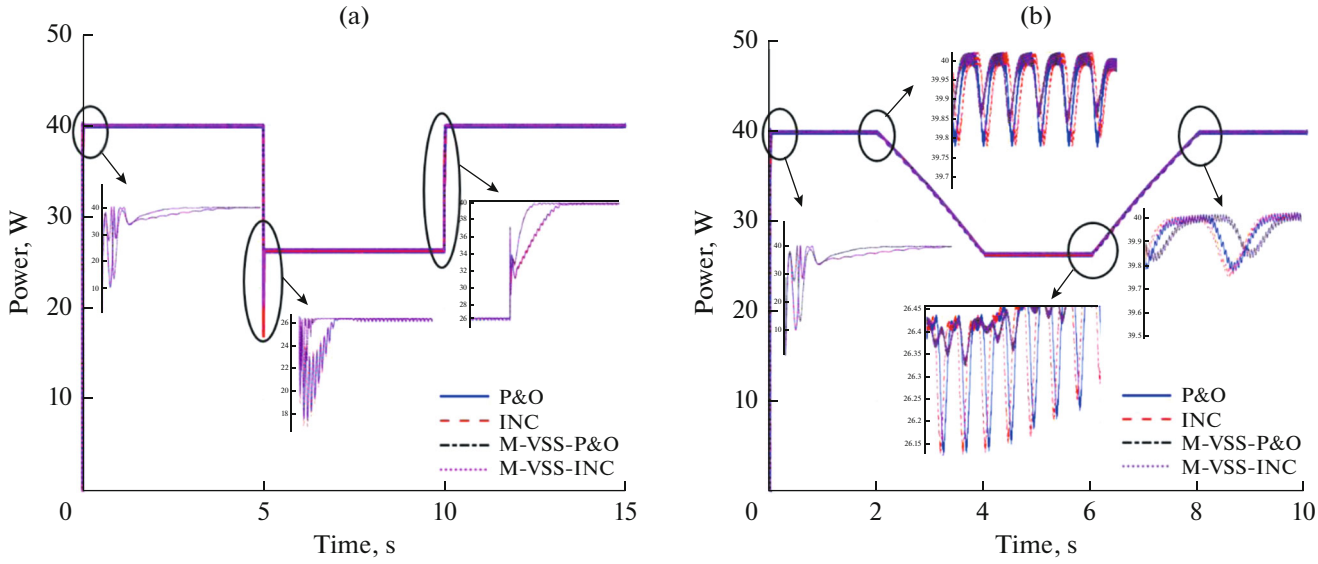

Fig. 15. Performance of thin film cell ST40 under sudden and ramp changes in irradiance.

seen in Fig. 14b, similar to the performance of the KC200GT solar cell, the modified algorithms show better performance and lesser oscillations level.

Finally, simulation results of the thin film ST40 solar cell are shown in Fig. 15. When the irradiance was suddenly decreased to 600 W/m^2, both P&O and INC algorithms succeed in tracking the MPP of 26.41 W with high oscillations. They both showed the same behavior with response time equal to 5.032 s; almost with 32 ms error, while both modified algorithms could converge to the peak point faster than the conventional techniques by the same response in 5.013 s with less error of (13 ms) and also could minimize the steady-state oscillations around the MPP.

Moreover, the modified algorithms could also detect with faster response the sudden increase in the solar irradiance with only 20 ms error and approximately the same power of 39.95 W. On the other hand, both P&O and INC could reach the peak point with an error of 50 ms.

According to Fig. 15b, it is noticed that P&O and INC algorithms are less efficient in dealing with ramp change in the irradiance and the modified algorithms succeed in tracking the MPP with lower oscillations.

From the simulations of the previous case studies, it is noticed that the conventional P&O performs with less efficiency among the three different cells and presents high oscillations to reach the maximum power point, also it is observed that INC algorithm gives precisely the same performance as P&O in the polycrystalline and monocrystalline cells, but it was better than the P&O in the thin film cell.

On the other side, in both KC200GT and SQ85 cells, modifications made to both P&O and INC MPPT algorithms showed the same performance, succeeded in improving the performance of the solar cell to get the maximum available power from the panel and reaching the MPP faster than the conventional algorithms with lower oscillations level as much as possible.

However, the ST40 solar cell simulations showed different behavior in tracking the MPP. According to the observed simulations, the M-VSS-INC gives the best algorithm with higher efficiency and lower oscillation level than the other three algorithms.

On the other hand, according to the simulations done in both sudden and ramp changes in the solar irradiance, both P&O and INC algorithm succeed in tracking the MPP presenting higher oscillations. In comparison, both modified algorithms M-VSS-P&O and M-VSS-INC performed better and faster with lower steady state power oscillations among the three types of solar cells.

CONCLUSIONS

This paper provides a comparative study between two common and famous MPPT algorithms; (perturb and observe (P&O) and incremental conductance (INC) techniques) against two modified versions of variable step size for both techniques; (M-VSS-P&O and M-VSS-INC) using boost DC-DC converter for three different types of solar cells (polycrystalline KC200GT, monocrystalline SQ85 and ST40 thin film solar cells). Within the context of this paper, simulations using MATLAB-SIUMULINK are carried out for PV systems containing the four algorithms, under both STC and different variations forms in solar irradiance. The obtained simulation results are very promising and proved in general that the modified MPPTs controller (M-VSS-P&O and M-VSS-INC) performances, in terms of efficiency, oscillations and the tracking speed of the MPP are much better than those of the conventional MPPT algorithms (P&O and INC). This work could be extended by changing the working environmental conditions. The four algorithms could be tested under different conditions not only in the incident solar irradiance but also in the ambient temperature. Moreover, these algorithms could be implemented practically, and the simulation results are validated against the experimental results.

FUNDING

This research has been funded by Research Deanship of University of Ha'il – Saudi Arabia through project number RG-191279.

ACKNOWLEDGMENTS

The authors thank Prof. Abdelhalim Zekry at Microelectronics Laboratory, Faculty of Engineering, Ain Shams University for his support.

REFERENCES

1. Bayrak, F., Ertürk, G., and Oztop, H.F., Effects of partial shading on energy and exergy efficiencies for photovoltaic panels, *J. Cleaner Prod.,* 2017, vol. 164, pp. 58–69.
2. Awad, A., Bazan, P., and German, R., Optimized operation of PV/T and micro-CHP hybrid power systems, *Technol. Econ. Smart Grids Sustainable Energy,* 2016, vol. 1, no. 2.
3. Singh, G.K., Solar power generation by PV (photovoltaic) technology: A review, *Energy*, 2013, vol. 53, pp. 1–13.
4. Hoseinzadeh, S. and Azadi, R., Simulation and optimization of a solar-assisted heating and cooling system for a house in Northern of Iran, *J. Renewable Sustainable Energy,* 2017, vol. 9, id. 045101.
5. Marinic-Kragic, I., Nižetic, S., et al., Analysis of flow separation effect in the case of the free-standing photovoltaic panel exposed to various operating conditions, *J. Cleaner Prod.*, 2018, vol. 174, pp. 53–64.
6. Nezhad, M.E.Y. and Hoseinzadeh, S., Mathematical simulation and optimization of a solar water heater for an aviculture unit using MATLAB/SIMULINK, *J. Renewable Sustainable Energy,* 2017, vol. 9, id. 063702.
7. Hoseinzadeh, S., Yargholi, R., Kariman, H. and Heyns, P.S., Exergoeconomic analysis and optimization of reverse osmosis desalination integrated with geothermal energy, *Environ. Prog. Sustainable Energy*, 2020, vol. 39, no. 5, id. e13405.
8. Hoseinzadeh, S., Zakeri, M.H., Shirkhani, A., and Chamkha, A.J., Analysis of energy consumption improvements of a zero-energy building in a humid mountainous area, *J. Renewable Sustainable Energy,* 2019, vol. 11, id. 015103.
9. Motahhir, S., El Ghzizal, A., Sebti, S., and Derouich, A., MIL and SIL and PIL tests for MPPT algorithm, *Cogent Eng.*, 2017, vol. 4, id. 1378475.
10. Zekry, A., Shaker, A., and Salem, M., Solar cells and arrays, in *Advances in Renewable Energies and Power Technologies,* Amsterdam: Elsevier, 2018, pp. 3–56.
11. El Hammoumi, A., Motahhir, S., Chalh, A., et al., Low-cost virtual instrumentation of PV panel characteristics using Excel and Arduino in comparison with traditional instrumentation, *Renewables: Wind, Water, Sol.*, 2018, vol. 5, art. no. 3.
12. Patel, H. and Agarwal, V., MATLAB-based modeling to study the effects of partial shading on PV array characteristics, *IEEE Trans. Energy Convers.*, 2008, vol. 23, no. 1, pp. 302–310.

13. Motahhir, S., El Ghzizal, A., Sebti, S., and Derouich, A., Proposal and implementation of a novel perturb and observe algorithm using embedded software, in *3rd International Renewable and Sustainable Energy Conference (IRSEC)*, 2015, pp. 1–5.

14. Ansari, B. and Simoes, M.G., Distributed energy management of PV-storage systems for voltage rise mitigation, *Technol. Econ. Smart Grids Sustainable Energy*, 2017, vol. 2, no. 1, p. 15.

15. Verma, D., Nema, S., Shandilya, A.M., and Dash, S.K., Maximum power point tracking (MPPT) techniques: Recapitulation in solar photovoltaic systems, *Renewable Sustainable Energy Rev.*, 2016, vol. 54, pp. 1018–1034.

16. El-Khozondar, H.J., El-Khozondar, R.J., Matter, K., and Suntio, T., A review study of photovoltaic array maximum power tracking algorithms, *Renewables: Wind, Water, Sol.*, 2016, vol. 3, art. no. 3.

17. Gupta, A., Chauhan, Y.K., Pachauri, R.K., Yin, X., and Pickert, V., A comparative investigation of maximum power point tracking methods for solar PV system, *Sol. Energy*, 2016, vol. 136, pp. 236–253.

18. Ahmed, J., A fractional open circuit voltage based maximum power point tracker for photovoltaic arrays, in *2nd International Conference on Software Technology and Engineering (ICSTE),* 2010, vol. 1, pp. V1–247.

19. Kottas, T.L., Boutalis, Y.S., and Karlis, A.D., New maximum power point tracker for PV arrays using fuzzy controller in close cooperation with fuzzy cognitive networks, *IEEE Trans. Energy Convers.*, 2006, vol. 21, no. 3, pp. 793–803.

20. Miloudi, L., Acheli, D., and Kesraoui, M., Application of artificial neural networks for forecasting photovoltaic system parameters, *Appl. Sol. Energy*, 2017, vol. 53, no. 2, pp. 85–91.

21. Sellami, A., Kandoussi, K., et al., A novel auto-scaling MPPT algorithm based on perturb and observe method for photovoltaic modules under partial shading conditions, *Appl. Sol. Energy*, 2018, vol. 54, no. 3, pp. 149–158.

22. Elgendy, M.A., Zahawi, B., and Atkinson, D.J., Assessment of perturb and observe MPPT algorithm implementation techniques for PV pumping applications, *IEEE Trans. Power Electron.*, 2012, vol. 3, no. 1, pp. 21–33.

23. Elgendy, M.A., Zahawi, B., and Atkinson, D.J., Assessment of the incremental conductance maximum power point tracking algorithm, *IEEE Trans. Sustainable Energy*, 2013, vol. 4, no. 1, pp. 108–117.

24. Motahhir, S., El Ghzizal, A., Sebti, S., and Derouich, A., Modeling of photovoltaic system with modified incremental conductance algorithm for fast changes of irradiance, *Int. J. Photoenergy*, 2018, vol. 2018, pp. 1–13. https://doi.org/10.1155/2018/3286479

25. Femia, N., Granozio, D., et al., Predictive & adaptive MPPT perturb and observe method, *IEEE Trans. Aerosp. Electron. Syst.,* 2007, vol. 43, no. 3, pp. 934–950.

26. Piegari, L. and Rizzo, R., Adaptive perturb and observe algorithm for photovoltaic maximum power point tracking, *IET Renewable Power Gener.*, 2010, vol. 4, no. 4, pp. 317–328.

27. Elbaset, A.A., Ali, H., Sattar, M., and Khaled, M., Implementation of a modified perturb and observe maximum power point tracking algorithm for photovoltaic system using an embedded microcontroller, *IET Renewable Power Gener.*, 2016, vol. 10, no. 4, pp. 1–10.

28. Motahhir, S., El Ghzizal, A., Sebti, S., and Derouich, A., Shading effect to energy withdrawn from the photovoltaic panel and implementation of DMPPT using C language, *Int. Rev. Autom. Control (IREACO)*, 2016, vol. 9, no. 2, pp. 88–94.

29. Ishaque, K., Salam, Z., and Lauss, G., The performance of perturb and observe and incremental conductance maximum power point tracking method under dynamic weather conditions, *Appl. Energy*, 2014, vol. 119, pp. 228–236.

30. Motahhir, S., Chalh, A., Ghzizal, A., Sebti, S., Derouich, A., Modeling of photovoltaic panel by using proteus, *J. Eng. Sci. Technol. Rev.*, 2017, vol. 10, no. 2, pp. 8–13. https://doi.org/10.1155/2018/3286479

31. Farayola, A.M., Hasan, A.N., and Ali, A., Implementation of modified incremental conductance and fuzzy logic MPPT techniques using MCUK converter under various environmental conditions, *Appl. Sol. Energy*, 2017, vol. 53, no. 2, pp. 173–184.

32. Elbreki, A.M., Alghoul, M.A., et al., The role of climatic-design-operational parameters on combined PV/T collector performance: A critical review, *Renewable Sustainable Energy Rev.,* 2016, vol. 57, pp. 602–647.

33. Jahan Mukti, R. and Islam, A., Modeling and performance analysis of PV module with maximum power point tracking in Matlab/Simulink, *Appl. Sol. Energy*, 2015, vol. 51, no. 4, pp. 245–252.

34. Aoune, A., Motahhir, S., El Ghzizal, A., Sebti, S., and Derouich, A., Determination of the Maximum Power Point in a photovoltaic panel using Kalman filter on the environment PSIM, *IEEE Int. Conf. on Information Technology for Organizations Development (IT4OD),* 2016, pp. 1–4.

35. Gow, J.A. and Manning, C.D., Development of a photovoltaic array model for use in power-electronics simulation studies, *lEE Proc. – Electr. Power Appl.*, 1999, vol. 146, no. 2, pp. 193–200.

36. Nishioka, K., Sakitani, N., Uraoka, Y., Fuyuki, T., et al., Analysis of multicrystalline silicon solar cells by modified 3-diode equivalent circuit model taking leakage current through periphery into consideration, *Sol. Energy Mater. Sol. Cells,* 2007, vol. 91, no. 13, pp. 1222–1227.

37. Ba, A., Ehsseinb, C.O., et al., Comparative study of different DC/DC power converter for optimal PV system using MPPT (P&O) method, *Appl. Sol. Energy*, 2018, vol. 54, no. 4, pp. 235–245.

38. Biswas, P.P., Suganthan, P.N., Wu, G., and Amaratunga, G.A.J., Parameter estimation of solar cells using datasheet information with the application of an adap-

tive differential evolution algorithm, *Renewable Energy*, 2018, vol. 132, pp. 425–438.

39. Louzazni, M. and Aroudam, El H., An analytical mathematical modeling to extract the parameters of solar cell from implicit equation to explicit form, *Appl. Sol. Energy*, 2015, vol. 51, no. 3, pp. 165–171.

40. Ayop, R. and Tan, C.W., Design of boost converter based on maximum power point resistance for photovoltaic applications, *Sol. Energy*, 2018, vol. 160, pp. 322–335.

41. Sanjaya, S., *Switching Power Supplies A to Z*, Boston: Newnes, 2006.

42. Al-Diab, A. and Sourkounis, S., Variable step size P&O MPPT algorithm for PV systems, *Int. Conf. on Optimization of Electrical and Electronic Equipment,* 2010.

43. Zakzouk, N.E., Elsaharty, M.A., Abdelsalam, A.K., Helal, A.A., and Williams, B.W., Improved performance low-cost incremental conductance PV MPPT technique, *IET Renewable Power Gener.*, 2016, vol. 10, no. 4, pp. 561–574.

44. Zhang, L., Yu, S.S., Fernando, T., Iu, H.C.H., and Wong, K.P., An online maximum power point capturing technique for high efficiency power generation of solar photovoltaic systems, *J. Mod. Power Syst. Clean Energy*, 2019, vol. 7, no. 2, pp. 357–368.